

RESEARCH ARTICLE

Small-molecule inhibition of pyruvate phosphate dikinase targeting the nucleotide binding site

Alexander Minges, Georg Groth*

Cluster of Excellence on Plant Sciences (CEPLAS), Institute of Biochemical Plant Physiology, Heinrich Heine University Düsseldorf, 40204 Düsseldorf, Germany

* georg.groth@hhu.de



Abstract

Pyruvate phosphate dikinase (PPDK) is an essential enzyme of C_4 photosynthesis in plants, catalyzing the ATP-driven conversion of pyruvate to phosphoenolpyruvate (PEP). It is further used by some bacteria and unicellular protists in the reverse, ATP-forming direction. Many weed species use C_4 photosynthesis in contrast to world's major crops, which are C_3 plants. Hence inhibitors of PPDK may be used as C_4 -specific herbicides. By screening a library of 80 commercially available kinase inhibitors, we identified compounds derived from bisindolylmaleimide (bisindolylmaleimide IV, $IC_{50} = 0.76 \pm 0.13 \mu M$) and indirubin (indirubin-3'-monoxime, $IC_{50} = 4.2 \pm 0.9 \mu M$) that showed high inhibitory potency towards PPDK and are among the most effective PPDK inhibitors described today. Physiological studies on leaf tissues of a C_4 model plant confirmed *in vivo* inhibition of C_4 -driven photosynthesis by these substances. Moreover, comparative docking studies of non-inhibitory bisindolylmaleimide derivatives suggest that the selectivity towards PPDK may be increased by addition of functional groups to the core structure.

OPEN ACCESS

Citation: Minges A, Groth G (2017) Small-molecule inhibition of pyruvate phosphate dikinase targeting the nucleotide binding site. PLoS ONE 12(7): e0181139. <https://doi.org/10.1371/journal.pone.0181139>

Editor: Qiming Jane Wang, University of Pittsburgh School of Medicine, UNITED STATES

Received: March 20, 2017

Accepted: June 27, 2017

Published: July 10, 2017

Copyright: © 2017 Minges, Groth. This is an open access article distributed under the terms of the [Creative Commons Attribution License](https://creativecommons.org/licenses/by/4.0/), which permits unrestricted use, distribution, and reproduction in any medium, provided the original author and source are credited.

Data Availability Statement: All relevant data are within the paper.

Funding: This work was supported by Heinrich Heine University Düsseldorf (scholarships within the iGRASPseed-Graduate Cluster for AM) (<http://igrasp.hhu.de/>).

Competing interests: The authors have declared that no competing interests exist.

Introduction

The main characteristic of C_4 plants is their ability to thrive in warm and dry environmental conditions by efficient usage of nitrogen, water and CO_2 [1–3]. This is ensured by spatial separation of the primary carbon fixation in mesophyll cells from CO_2 release to the Calvin-Benson Cycle in the bundle sheet cell chloroplasts, leading to a much more efficient carbon fixation compared to C_3 plants, where primary carbon fixation takes place directly in the Calvin-Benson Cycle [4].

Many of today's crops, such as wheat or rice, use the C_3 pathway, while most of the world's worst weeds (e.g. *Cyperus rotundus* or *Echinochloa crus-galli*) are C_4 plants [5]. Hence, an herbicide that specifically targets C_4 plants would be of highest interest to ensure high crop yields in the context of increasing resistances against conventional herbicides. A potential target of the C_4 photosynthetic pathway is pyruvate phosphate dikinase (PPDK) which is one of the rate limiting enzymes of C_4 photosynthesis [6]. It catalyzes the ATP-driven interconversion of

pyruvate to phosphoenolpyruvate (PEP) and hereby regenerates PEP that is used as the primary CO₂ acceptor in C₄ plants. PPDK is composed of three distinct domains with well-defined functionalities (all residue numbers according to *Flaveria trinervia* notation): An N-terminal nucleotide binding domain (NBD, aa 1–340), a central domain (CD, aa 381–516) and a C-terminal PEP/pyruvate binding domain (PBD, aa 534–874). The CD is linked to both substrate binding domains via two flexible linker regions (aa 341–380 and aa 517–533) and includes the catalytic His456 residue which is used in the transfer of a phosphoryl group from the nucleotide substrate ATP bound to the NBD to pyruvate at the PBD and vice versa. This phospho-transfer has to bridge a distance of approx. 40 Å from one substrate binding site to the other. Hence a swiveling domain mechanism was proposed to explain the large rotational and translational movement of the CD required for phosphoryl group transfer between the two catalytic centers [7, 8]. This swiveling mechanism has been supported by X-ray crystallographic data of PPDKs from *Clostridium symbiosum*, *Trypanosoma brucei* and *Zea mays*, which have resolved two extreme conformations of the CD—one facing the NBD, the other one facing the PBD [7, 9, 10]. A recently resolved structure of PPDK from the C₄ plant *F. trinervia*, representing a conformational intermediate of the catalytic cycle, illustrates that the proposed CD swiveling motion proceeds via at least one discrete sub-step [11]. Thus, similar to other proteins employing large domain movements such as the F₁-ATPase or the bacterial flagellar motor, PPDK also seems to operate discrete sub-steps in the movement of the CD associated with the catalytic cycle.

Catalytic activity of PPDK is regulated by phosphorylation of a threonine residue (aa 454 in *Flaveria*), located in close proximity to the catalytic histidine (aa 456 in *Flaveria*). Remarkably, both phosphorylation and dephosphorylation of the regulatory threonine are catalyzed by a bifunctional enzyme, the PPDK regulatory protein (PPDK-RP) [12–15]. In plants, activation and inactivation of PPDK by PPDK-RP are light-mediated and depend on ADP and AMP levels at dark and light periods. High levels of stromal ADP stimulate phosphorylation in the dark and at the same time inhibit dephosphorylation of the regulatory threonine [14, 16]. The three-dimensional structure of PPDK-RP from *Zea mays* has been recently solved, providing insights into the unusual bifunctionality of this protein [17].

While PPDK is essential for all C₄ plants, it is not crucial for C₃ plants: PPDK knock-out mutants of *Oryza sativa* and *Arabidopsis thaliana* grown under normal environmental conditions do not exhibit any obvious phenotypical anomalies [18, 19]. Moreover, although PPDK is used by some bacteria and unicellular parasitic protists such as *Giardia lamblia*, *Trichomonas vaginalis*, or *Entamoeba histolytica*, no homologue of PPDK is known in insects or vertebrates. This absence in higher animals makes PPDK an interesting target for antimicrobial and anti-parasitic drugs as well as C₄-specific herbicides.

Past studies have identified several substances originating from marine organisms with inhibitory effects on PPDK [20–23]. Among these, hydroxyquinones, ilimaquinone, ethylsmenoquinone and smenoquinone showed inhibitory constants in the higher micromolar range. The mode of action of these compounds is still not fully understood. In some cases, a mixed-type inhibition with regard to ATP was reported, which may hint at a binding at or near the nucleotide binding side. In a more recent study by Wu *et al.* [24], the nucleotide binding site was targeted directly by tight binding, space-filling flavone derivatives, resulting in a number of hits with high inhibitory potency and specificity towards PPDK.

Building on these results, the search of novel inhibitors of PPDK may not only focus on the ATP binding site as a primary—but often neglected as “generic”—target, but may also include known kinase inhibitors. In a similar attempt, Armstrong *et al.* [25] successfully identified inhibitors of carbohydrate sulfotransferase using a library of known kinase inhibitors. Here we report on the identification of novel high-potency inhibitors of PPDK targeting the nucleotide

binding site from a set of commercially available kinase inhibitors by using PPDK from the C₄ plant *Flaveria trinervia* in an *in vitro* assay. Further studies on leaf tissues of the C₄ model plant maize demonstrate that these compounds inhibit C₄-driven photosynthesis *in vivo* and confirm that these substances inhibit PPDK at naturally occurring enzyme and substrate concentrations.

Materials and methods

Heterologous expression and protein purification

Heterologous gene expression and purification of the recombinant PPDK were performed as described in [11]. A modified pET-16b vector (Merck, Darmstadt, GER) which contained an N-terminal histidine₁₀ tag, followed by a TEV cleavage site and the sequence encoding for PPDK from *Flaveria trinervia* (EMBL X75516) was used for heterologous expression in *E. coli* strain BL21 (DE3). Transformed cells were grown to an OD₆₀₀ of 0.6–0.8 in 2YT medium at 30°C before expression was induced by the addition of 0.1 mM isopropyl-β-D-1-thiogalactopyranoside. Cells were harvested after over night incubation at 30°C and 180 rpm. Preceding purification, cells were resuspended in lysis buffer (50 mM Tris/HCl pH 7.5, 300 mM NaCl, 10 mM imidazole, 10 mM MgSO₄, 10% (w/v) glycerol, 5 mM DTT, 0.002% (w/v) phenylmethanesulfonylfluoride) and disrupted using a cell disruptor (Constant Systems). PPDK was purified using a nickel affinity chromatography column (GE Healthcare, Munich, GER). Purification (50 mM Tris/HCl pH 7.5, 300 mM NaCl, 10 mM MgSO₄, 10% (w/v) glycerol, 5 mM DTT) and elution buffer (50 mM Tris/HCl pH 7.5, 300 mM NaCl, 500 mM imidazole, 10 mM MgSO₄, 10% (w/v) glycerol, 5 mM DTT) were used for further purification steps. PPDK bound to the column was washed in steps of 50 mM, 150 mM and 200 mM imidazole, before final elution with 500 mM imidazole. Protein-rich fractions were pooled and a PD-10 desalting column (GE Healthcare) was used to change the elution buffer for assay buffer (100 mM Tris/HCl pH 8.0, 10 mM MgCl₂, 2.5 mM KH₂PO₄, 6 mM glucose-6-phosphate, 5 mM NaHCO₃, 0.1 mM EDTA, 5 mM DTT). The buffer-exchanged sample was eventually concentrated by ultrafiltration (30 kDa cutoff, Millipore).

PPDK activity assay and inhibitor screening

A set of 80 compounds from a commercially available kinase inhibitor library (#10505; Cayman Chemicals, Ann Arbor, MI, USA) was screened for its effects on *F. trinervia* PPDK. Activity of purified PPDK was measured according to Salahas *et al.* [26], Doyle *et al.* [20] in a 96 well microtiter plate layout by a coupled spectrophotometrical assay. In this assay, the carboxylation of PEP by PEPC is linked to the oxidation of NADH by NADH-malate dehydrogenase (NADH-MDH). PEP is formed by PPDK via ATP-driven phosphorylation of pyruvate. Eventually, the consumption of one molecule NADH is equivalent to the formation of one molecule of PEP by PPDK. The assay was performed in a sample volume of 100 μL at 30°C in a M200 plate reader (Tecan, Crailsheim, GER). 0.2 μM PPDK were mixed with 0.2 mM NADH, 2.5 mM sodium pyruvate, 0.8 U bacterial PEPC (Sigma-Aldrich, Darmstadt, GER) and 2 U NADH-MDH (Sigma-Aldrich). The reaction mixture was filled up to a total volume of 100 μL per sample with assay buffer (100 mM Tris/HCl pH 8.0, 10 mM MgCl₂, 2.5 mM KH₂PO₄, 6 mM glucose-6-phosphate, 5 mM NaHCO₃, 0.1 mM EDTA, 5 mM DTT). PPDK was pre-incubated for 20 min at 30°C to ensure full activity. Inhibitors were dissolved in water free dimethyl sulfoxide (DMSO) with a final concentration of 10 mM and were added prior to adjusting the final sample volume. To account for possible effects of DMSO on PPDK activity, the solvent was added to the controls in an amount equal to the largest DMSO concentration used in the experiments. Incubation time of the final sample mixture including inhibitors and

PPDK was 15 min. Initial comparative screening was performed using 100 μM of each compound. The absorbance at 340 nm was recorded for 30 s with an interval of 300 ms. The reaction was started by automated injection of 1.25 mM ATP. The activity was then deduced from the initial slope, discarding the first 10 s due to noise caused by mixing effects and normalized to the DMSO-treated controls. Six compounds with the highest potency were chosen for further analysis of their inhibitory potential. Since compounds of the bisindolylmaleimide class showed similar effects on PPDK activity, only two of them (BIM IV and Go6983) were chosen as representatives of this class. The half maximal (50%) inhibitory concentration IC_{50} of the selected compounds was calculated by measuring the activity as described before for at least ten data points in the concentration range of 0 μM to 200 μM of the inhibitory compound in at least triplicates. A four-parameter log-logistic dose-response curve was then globally fitted to the individual replicates using the R software collection [27] and the R package “drc” [28] as proposed by assessment of Akaike’s information criterion (AIC) [29, 30]. PPDK was incubated for 10 min with the inhibitors before each measurement. To exclude PEPC or NADH-MDH inhibition by the selected compounds, the initial screening assay was repeated in triplicates for those compounds without adding PPDK and starting the reaction by injection of PEP instead of ATP. Determined activities were compared to the control and statistically analyzed using a paired t-test.

Inhibition of oxygen evolution during C₄ photosynthesis

Oxygen (O₂) evolution, driven by the C₄ acid cycle, was measured according to refs [21, 22, 31]. The reaction chamber of a Clark-type O₂ electrode (Hansatech, Norfolk, UK) was filled with 1 mL of degassed buffer containing 0.33 M sorbitol, 2.5 mM NaH₂PO₄, 2.5 mM MgCl₂, 25 mM HEPES/KOH pH 7.5, 50 μM MnCl₂ and 2.5 mM dithiothreitol (DTT). An area sized approx. 1 cm² was cut from a mature leaf of the C₄ model plant *Zea mays* and processed into slices of ~ 1 mm width. The leaf slices were added to the electrode chamber and the recording of O₂ evolution was started while keeping the chamber in the dark. The O₂ evolution rate recorded in this period was later subtracted from the subsequently recorded rates to account for the electrode drift. Once the system had stabilized, the chamber was illuminated using a Schott KL 1500 electronic light source. Again, the system was given time to stabilize before the C₄-driven O₂ evolution was initiated by the addition of first NaHCO₃ and then pyruvate in final concentrations of 4 mM each. In agreement with [21], the NaHCO₃-dependent O₂ evolution rate was negligible. The O₂ evolution rate after adding pyruvate was recorded for at least 3 min after it had stabilized and was used as the control rate. Then a total amount of 20 μg and 40 μg (if possible due to solubility limit) of the test substance dissolved in DMSO was added to the reaction chamber and the O₂ evolution rate was again recorded for at least 3 min. All measurements were done in triplicates.

Directly following the measurement, leaf slices were removed from the chamber and transferred to 1 mL of 80% acetone (v/v) for chlorophyll extraction. The samples were kept at 4°C in the dark for 48 h. The total chlorophyll amount was determined using a DU800 (Beckman Coulter, USA) spectrophotometer and calculated using Eq (1) [32].

$$\text{total chl } [\mu\text{g mL}^{-1}] = (20.2 \times OD_{645}) + (8.02 \times OD_{663}) \quad (1)$$

The O₂ evolution rates in the presence of the inhibitors were compared to the respective controls and statistically analyzed using a two-sided t-test. Relative inhibition of O₂ evolution was

expressed in percent and calculated as stated in Eq (2).

$$\text{inhibition [\%]} = 100 - \frac{\text{O}_2 \text{ evolution treated} \times 100}{\text{O}_2 \text{ evolution control}} \quad (2)$$

Docking of compounds into the nucleotide binding site

Since all of the most-inhibiting compounds are described as inhibitors for nucleotides or nucleic acids in their original targets, virtual docking of these molecules was performed into the ATP binding cleft of PDB 5JVL chain D. The bounding box was sized 20 Å in each dimension and centered at the position of the 4'-carbon atom of the nucleotide analogue 2'-Br-dAppNHp bound to this structure. 2'-Br-dAppNHp was removed after filling missing side-chains using a rotamer library [33] and protonation with tools from UCSF Chimera [34]. A maximum of 200 conformers of each compound was generated using RDKit [35]. Conformers with RMSDs below 0.1 Å to other conformers in the same set were discarded. Those sets of conformers were docked with the AutoDock Vina-derived program smina [36, 37]. The docked results were then ranked according to their predicted binding energy. Images were prepared using PyMOL [38]

Results and discussion

To search for inhibitory compounds blocking the nucleotide binding site, a set of 80 commercially available kinase inhibitors was screened for effects on PPDK from the C₄ plant *Flaveria trinervia*. Analysis of the initial test set by plotting the residual PPDK activity after inhibitor treatment revealed several promising candidates. Of the 80 tested compounds, 22 led to 50% inhibition of PPDK activity at a concentration of 100 μM. Eleven of the tested compounds reduced the activity even to levels below 30%. Seven of the top scoring compounds belong to the chemical class of bisindolylmaleimides which are characterized by an indol-substituted maleimide structure and varying other structural elements. Six of the bisindolylmaleimide compounds caused an almost complete loss of PPDK activity when applied at concentrations of 100 μM. Residual activity measured was in the range of 1–3% of the DMSO-treated controls except for bisindolylmaleimide V showing a residual activity of 15% (Fig 1). Compounds of the bisindolylmaleimide class have been previously identified as high-potency inhibitors of human protein kinase C (PKC) with IC₅₀ values in the nanomolar range [39–42]. A second class of PPDK inhibitors is formed by indirubin-3'-monoxime (IO) and its bromized derivative 6-bromoindirubin-3'-monoxime (BIO), which are described as ATP-competitive inhibitors of cyclin-dependent kinases (CDK, IC₅₀: 50–100 nM) and glycogen synthase kinase 3β (GSK3β, IC₅₀: 5–50 nM) [43, 44]. However, residual activities observed after treatment with this chemical class were up to two-fold higher than with the bisindolylmaleimides. The other remaining compounds identified in our screening reducing PPDK activity below 30% (Fig 1) – ABT-869 and PP242 – are not structurally related to each other or to the two other groups. Both are ATP-competitive inhibitors, targeting receptor tyrosine kinases (RYK, ABT-869) and mammalian target of rapamycin (mTOR, PP242) with IC₅₀ values of 4 nM and 8 nM, respectively [45, 46].

To exclude the possibility that the inhibitors identified in our screening target PEPC or NADH-MDH and thereby bias the coupled enzymatic assay, the assay was repeated in the absence of PPDK and ATP and the reaction was started by the addition of PEP. Hence, only inhibitory effects on either PEPC or NADH-MDH were addressed in this experimental setup. The results were compared with those of the controls and statistically analyzed. Only for BIO,

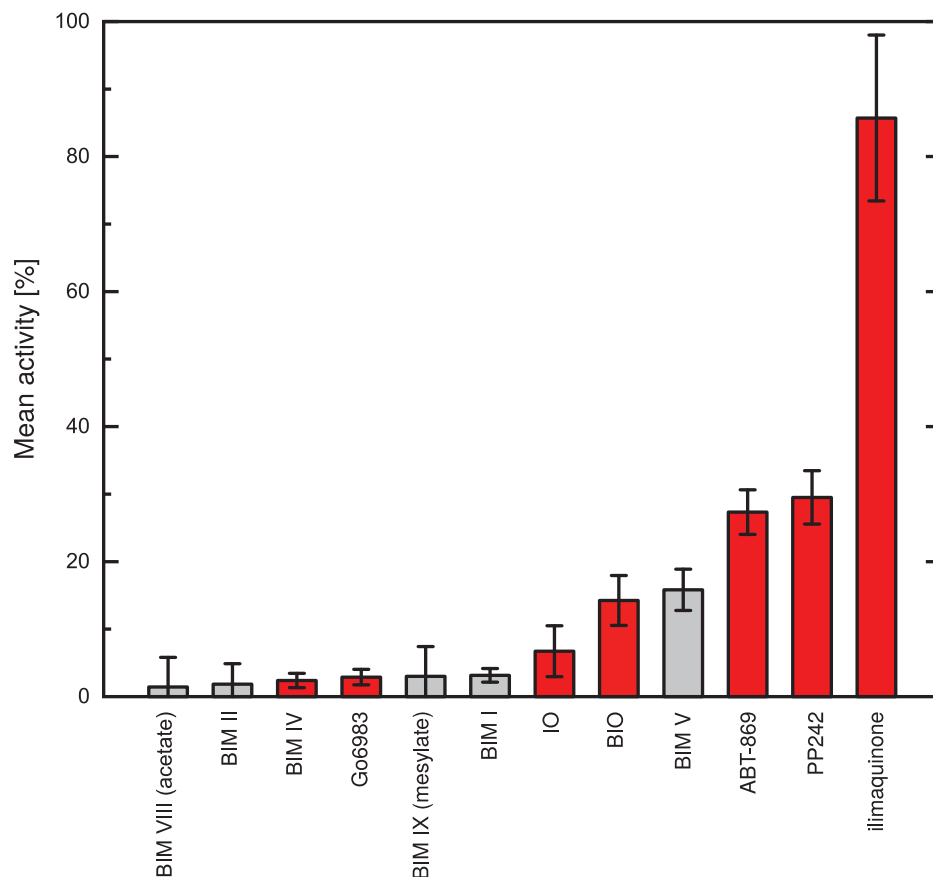


Fig 1. Mean activity of PPDK at inhibitor concentrations of 100 µM. Depicted from left to right are the most potent inhibitors identified in the initial screening assay with the known PPDK inhibitor ilimaquinone. Inhibitors colored red were further analyzed for their IC_{50} values. Errors shown are standard deviations (SD).

<https://doi.org/10.1371/journal.pone.0181139.g001>

a significant inhibition of PEPC or NADH-MDH was apparent (data not shown). The remaining activity was still well above 60% of the control. Therefore it is unlikely that the drop of PPDK activity observed for BIO to about 15% is caused by PEPC or NADH-MDH inhibition alone, but is mainly caused by inhibition of PPDK. For all other compounds, no significant inhibition of PEPC or NADH-MDH was detected.

The IC_{50} of the two indirubines, ABT-869, PP242, bisindolylmaleimide IV (BIM IV) and Go6983 were experimentally determined (Fig 2). For comparison, the PPDK specific inhibitor ilimaquinone [21] was added to the test set. In accordance to the measured activities from the initial screening, the two bisindolylmaleimides, BIM IV and Go6983, performed best with IC_{50} values (mean \pm standard error) of 0.76 ± 0.13 µM and 1.5 ± 0.6 µM, respectively. An about ten-fold lower inhibitory potency was shown by the two indirubines. The IC_{50} of IO was determined at 4.2 ± 0.9 µM. The bromized form showed an even higher value of 11.3 ± 0.8 µM. The IC_{50} of ABT-869 and PP242 were more than 10-fold higher than those of the two bisindolylmaleimides with 11.2 ± 0.24 µM and 16.2 ± 0.32 µM. The PPDK-specific inhibitor ilimaquinone was the least potent inhibitor in this series with an IC_{50} of 740 ± 566 µM (Fig 3). In total, the inhibitory potency of the bisindolylmaleimides identified in this study is comparable and in case of BIM IV even higher than for the alkyl-substituted flavonoids previously described by Wu *et al.* [24].

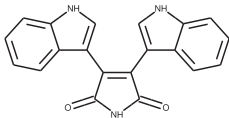
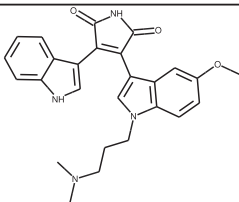
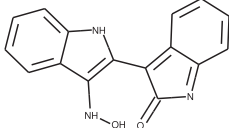
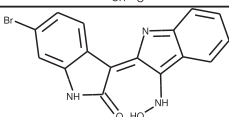
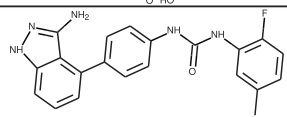
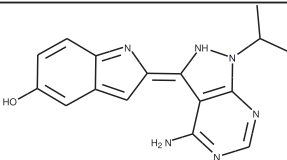
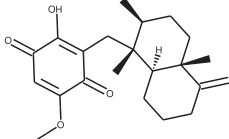
Compound	Structure	<i>IC</i> ₅₀ [μM]
bisindolylmaleimide IV		0.76 ± 0.13
Go6983		1.5 ± 0.6
indirubin-3'-monoxime		4.2 ± 0.9
6-bromoindirubin-3'-monoxime		11.3 ± 0.8
ABT-869		11.2 ± 2.4
PP242		16.2 ± 3.2
ilimaquinone		740 ± 566 292 ± 23 ^a

Fig 2. Structures and *IC*₅₀ values of PPK inhibitors. ^a *IC*₅₀ of ilimaquinone measured for *Zea mays* PPK from leaf extracts according to Haines *et al.* [21]. Errors shown are standard errors (SE).

<https://doi.org/10.1371/journal.pone.0181139.g002>

A primary obstacle for postemergent herbicides clearly is their uptake into the plant, particularly penetration of the leaf cuticle [47]. Consequently, the exact formulation of adjuvants to promote leaf penetration is one of the major issues in herbicide research and development. However, once inside the leaf, the extensive network of plasmodesmata in the bundle sheet cells of C₄ plants facilitates further spreading of the applied chemical. In leaf slice assays, the cuticular barrier is bypassed by direct exposure of parts of the plasmodesmata to the surrounding buffer while keeping the integrity of the intra- and intercellular C₄ photosynthetic apparatus intact. This allows to study the effect of inhibitors in a native cellular milieu. To substantiate the results of our *in vitro* assay and to elaborate the effect of the compounds identified in this assay under *in vivo* conditions, we thus applied oxygen measurements on isolated leaf slices of the C₄ model plant maize.

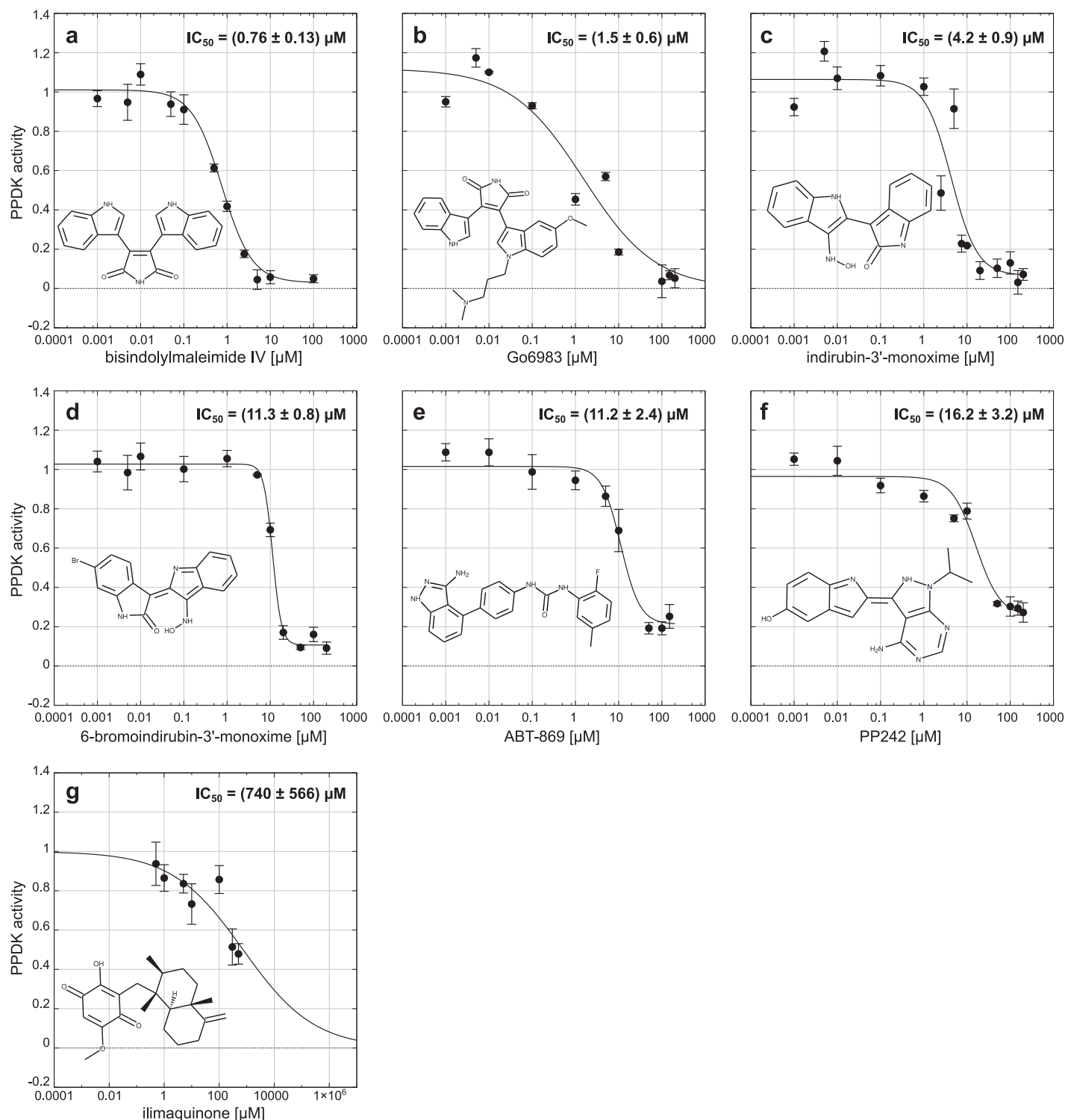


Fig 3. Dose-response curves of selected inhibitors of C₄ plant PPK. The PPK concentration is kept constant at 0.2 μM , while the inhibitor concentrations are varied between 0 μM and 200 μM . The mean activity from three experiments relative to the control is plotted for bisindolylmaleimide IV (a), Go6983 (b), indirubin-3'-monoxime (c), 6-bromoindirubin-3'-monoxime (d), ABT-869 (e), PP242 (f) and the PPK specific inhibitor ilimaquinone (g). The IC_{50} values were calculated from these data by non-linear regression using log-logistic dose-response functions. Errors shown are standard errors of the mean (SEM).

<https://doi.org/10.1371/journal.pone.0181139.g003>

Of the six putative PPKD inhibitors characterized in the *in vitro* assay, five led to a significant decrease in C₄-dependent O₂ evolution rate (Fig 4). Two of them (IO and BIO) even show negative rates, representing a dramatic net O₂ consumption. However, both compounds include an oxime group structure, known to scavenge molecular oxygen from aqueous solutions [48]. Thus, the O₂ consumption observed with IO and BIO is probably related to a chemical rather than a biological effect.

For the remaining three inhibitors with significant effects on the O₂ evolution rate, BIM IV inhibits O₂ evolution by 20% when applied at a final concentration of 20 µg mL⁻¹ and 36% at 40 µg mL⁻¹. Similarly, the inhibition observed for Go6983 is 19% at 20 µg mL⁻¹ and 29% at 40 µg mL⁻¹. Due to its solubility limit, PP242 was only applied at 20 µg mL⁻¹. However, already at this concentration, 73% inhibition of photosynthetic oxygen evolution was observed (Fig 4).

Remarkably, although the bisindolylmaleimides seem to represent the best inhibitors tested in this study, one representative of this family (bisindolylmaleimide XI, BIM XI) did not show any effect on PPKD activity at all. In contrast to other bisindolylmaleimides, this compound contains a rather bulky cyclo-hexyl structure attached at one of its indole groups. This bulky extension may lead to steric clashes between the compound and the amino acid residues forming the nucleotide binding pocket. To test this hypothesis, an *in silico* docking approach was taken, and the eleven initial top scoring compounds, including the seven most effective bisindolylmaleimides, were docked into the nucleotide binding site of the high resolution PPKD structure of *F. trinervia* (PDB 5JVL chain D) [11]. Predicted binding energies for the bisindolylmaleimides were in the range of -10.5 Kcal mol⁻¹ to -8.0 Kcal mol⁻¹ thus reflecting a relatively tight binding which is in accordance with our activity assays. In addition, similar docking poses of all bisindolylmaleimides in regard to their core structural features were identified among the top-rated docking poses. Superimposition of BIM XI with those consensus poses revealed severe clashes with the surrounding protein structure at the highly-conserved residues Arg95 and Glu324 (Fig 5a), confirming our hypothesis that clashes resulting in unfavorable interactions with the surrounding binding pocket prevent inhibition of PPKD in case of BIM XI. Analysis of the influence of Arg95 and Glu324 on BIM XI binding by substitution mutagenesis is hampered as both residues are directly involved in ATP substrate binding. Hence, a mutation of these residues is likely to abolish PPKD activity. Additional structural information on the exact binding mode of bisindolylmaleimides by means of crystal structures in the presence of these compounds are probably needed to answer this question. In their original target PKC, bisindolylmaleimides are known to bind at the same position as the natural substrate ATP [49, 50]. Similarly, our docking results suggest that the binding mode of bisindolylmaleimides in PPKD largely overlaps with the bound nucleotide analogue in PPKD structure 5JVL [11] (Fig 5b).

In summary, we were able to identify novel high-potency inhibitors of PPKD by screening a kinase inhibitor library. The novel inhibitors, which belong to the chemical classes of bisindolylmaleimides and indirubins, are among the most effective inhibitors of PPKD, with BIM IV as the single most potent PPKD inhibitor identified today. The compounds have been previously described as specific inhibitors of protein kinase C (PKC) and other kinases involved in cancer development. The herbicidal potential of the novel PPKD inhibitors is substantiated by *in vivo* plant studies, which show significant inhibition of C₄-dependent O₂ evolution by BIM IV, Go6983 and PP242. Their relatively high potency with IC₅₀ values in the higher nanomolar to lower micromolar range suggests that these compounds are interesting lead structures for further adaption to the PPKD nucleotide binding pocket. The fact that the extent and selectivity of PPKD inhibition indeed can be adapted by substitutions at the bisindolylmaleimide core is reflected by the observation that BIM XI shows no effect on PPKD activity due to potential steric clashes with amino acid side chains in the nucleotide binding pocket of PPKD.

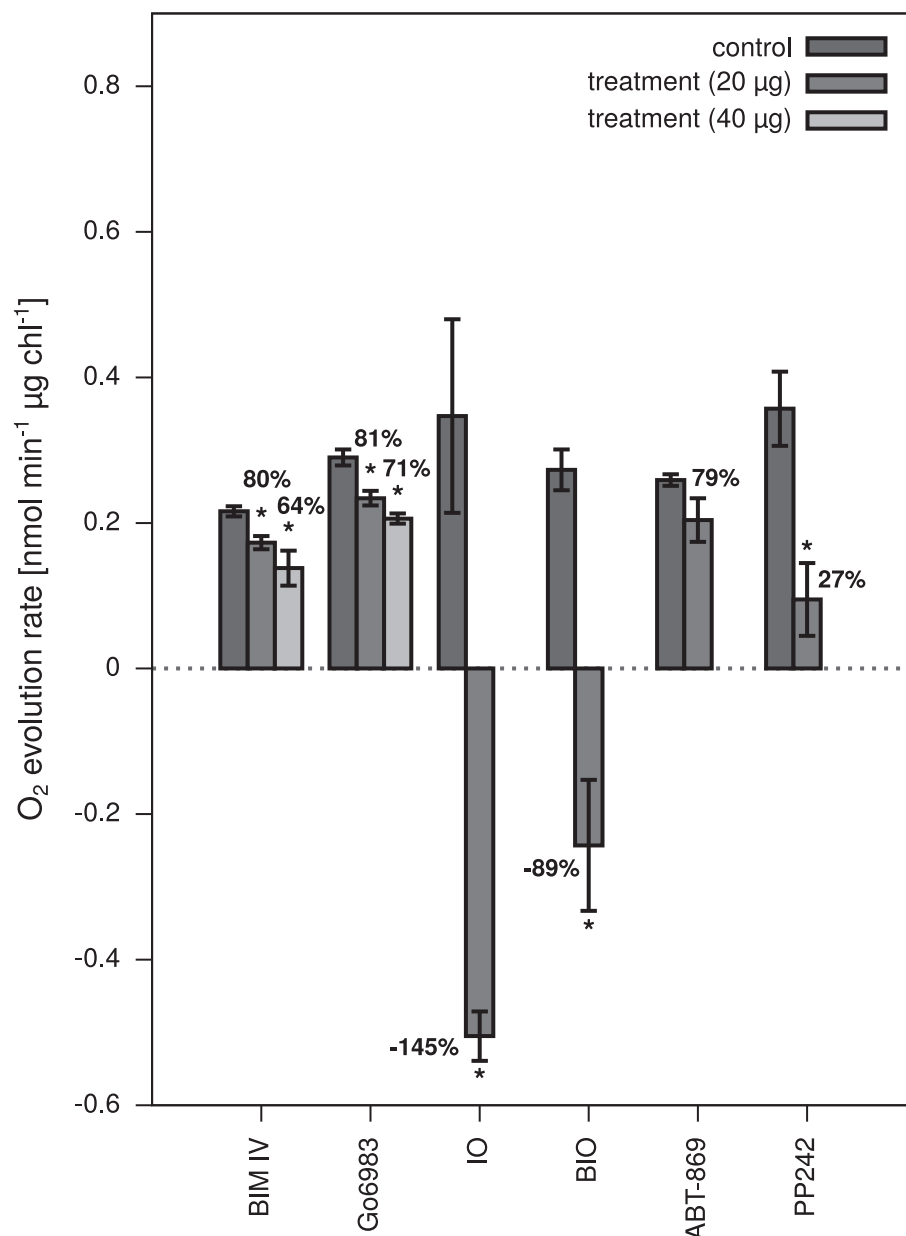


Fig 4. Oxygen evolution *in vivo* in the presence of putative PPDK inhibitors. The rate of O₂ evolution of *Zea mays* leaf slices was measured in solution with a Clark-type electrode. PPDK inhibitors identified in the *in vitro* screening assay were added to the leaf slices in a final concentration of 20 µg mL⁻¹. A significant decrease ($p \leq 0.05$) was observed for BIM IV, IO, BIO and PP242. Rates were normalized to the total amount of chlorophyll in the leaf samples and corrected for electrode drift. O₂ evolution rates relative to the respective controls are given in percent. Noteworthy, the O₂ evolution rate in the presence of IO and BIO was negative, hence representing a consumption of O₂. Errors shown are SEM.

<https://doi.org/10.1371/journal.pone.0181139.g004>

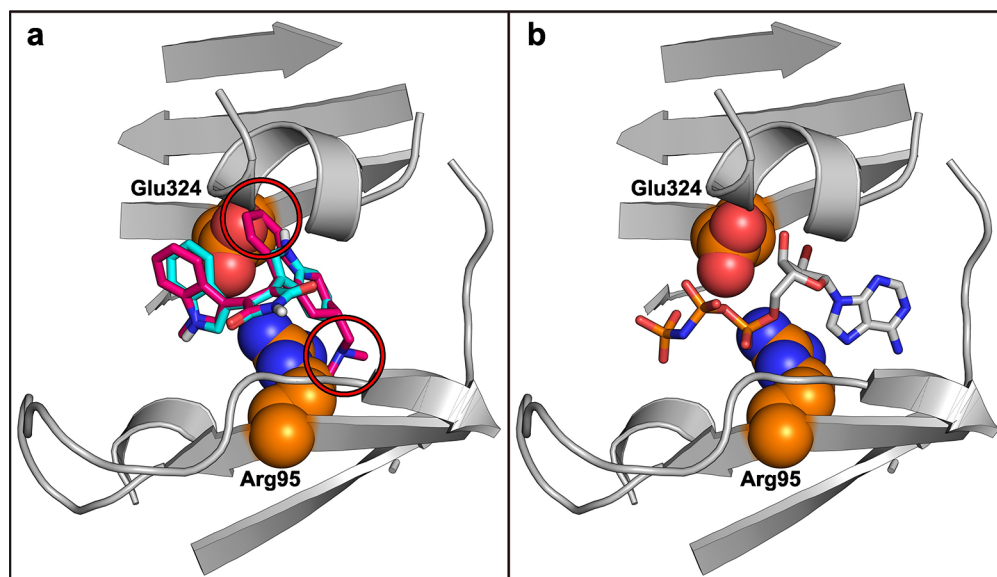


Fig 5. Predicted binding position of inhibitory and non-inhibitory bisindolylmaleimides at the nucleotide binding site of C₄ plant PPDK. (a) Bisindolylmaleimide IV (cyan) docked to the nucleotide binding domain of PPDK (PDB 5JVL chain D). Only parts of the whole structure are shown for clarity. Almost identical binding poses are among the top-rated docking results of all bisindolylmaleimides tested and proven to be effective in this study. The structure of the related but non-inhibitory compound bisindolylmaleimide XI is shown in magenta. Severe clashes of this compound occur with residues Arg95 and Glu324 and are highlighted by red circles. (b) Bound nucleotide analogue 2'-Br-dAppNHp in 5JVL chain D.

<https://doi.org/10.1371/journal.pone.0181139.g005>

Because the newly identified PPDK inhibitors were originally designed for other kinases such as the PKC, they do not exclusively target PPDK in their current structure and chemical composition. However, this may be addressed in further studies by evolving bisindolylmaleimides towards tighter and more specific interaction with the PPDK's nucleotide binding pocket while preserving their unprecedented inhibitory potential. Similar strategies have been successfully pursued in the past in the development of selective protein kinase inhibitors such as AMG706 for vascular endothelial growth factor receptor (VEGFR), PF-562271 for focal adhesion kinase (FAK) or GSK461364A for Polo-like kinase (PLK1) [51].

Acknowledgments

We thank our colleague Dr. Dalibor Milic for critical reading of the manuscript. This work has been supported by Heinrich Heine University Düsseldorf (scholarship within the iGRASP_{seed}-Graduate Cluster for AM).

Author Contributions

Conceptualization: Georg Groth.

Investigation: Alexander Minges.

Project administration: Georg Groth.

Visualization: Alexander Minges.

Writing – original draft: Alexander Minges, Georg Groth.

Writing – review & editing: Alexander Minges, Georg Groth.

References

1. Moore R, Black CC. Nitrogen Assimilation Pathways in Leaf Mesophyll and Bundle Sheath Cells of C₄ Photosynthesis Plants Formulated from Comparative Studies with *Digitaria sanguinalis* (L.) Scop. *Plant physiology*. 1979; 64(2):309–313. <https://doi.org/10.1104/pp.64.2.309> PMID: 16660955
2. Kopriva S. Nitrogen and Sulfur Metabolism in C₄ Plants. In: Raghavendra AS, Sage RF, editors. *C₄ Photosynthesis and Related CO₂ Concentrating Mechanisms*. Springer Netherlands; 2011. p. 109–123.
3. Ghannoum O, Evans JR, von Caemmerer S. Nitrogen and Water Use Efficiency of C₄ Plants. In: Raghavendra AS, Sage RF, editors. *C₄ Photosynthesis and Related CO₂ Concentrating Mechanisms*. Springer Netherlands; 2011. p. 129–146.
4. Hatch MD. C₄ photosynthesis: discovery and resolution. *Photosynthesis Research*. 2002; 251(73):251–256. <https://doi.org/10.1023/A:1020471718805>
5. Holm LG, Plucknett DL, Pancho JV, Herberger JP, et al. *The World's Worst Weeds: Distribution and Biology*. University of Hawaii Press; 1977.
6. Lawyer AL, Kelley SR, Allen JL. Use of pyruvate-phosphate dikinase as a target for herbicide design: analysis of inhibitor specificity. *Zeitschrift für Naturforschung C*. 1987; 42(7-8):834–836.
7. Herzberg O, Chen CC, Kapadia G, McGuire M, Carroll LJ, Noh SJ, et al. Swiveling-domain mechanism for enzymatic phosphotransfer between remote reaction sites. *Proceedings of the National Academy of Sciences of the United States of America*. 1996; 93(7):2652–7. <https://doi.org/10.1073/pnas.93.7.2652> PMID: 8610096
8. Lim K, Read RJ, Chen CCH, Tempczyk A, Wei M, Ye D, et al. Swiveling domain mechanism in pyruvate phosphate dikinase. *Biochemistry*. 2007; 46(51):14845–53. <https://doi.org/10.1021/bi701848w> PMID: 18052212
9. Cosenza LW, Bringaud F, Baltz T, Vellieux FMD. The 3.0Å Resolution Crystal Structure of Glycosomal Pyruvate Phosphate Dikinase from *Trypanosoma brucei*. *Journal of Molecular Biology*. 2002; 318(5):1417–1432. [https://doi.org/10.1016/S0022-2836\(02\)00113-4](https://doi.org/10.1016/S0022-2836(02)00113-4) PMID: 12083528
10. Nakanishi T, Nakatsu T, Matsuoka M, Sakata K, Kato H. Crystal structures of pyruvate phosphate dikinase from maize revealed an alternative conformation in the swiveling-domain motion. *Biochemistry*. 2005; 44(4):1136–44. <https://doi.org/10.1021/bi0484522> PMID: 15667207
11. Minges A, Ciupka D, Winkler C, Höppner A, Gohlke H, Groth G. Structural intermediates and directionality of the swiveling motion of Pyruvate Phosphate Dikinase. *Scientific Reports*. 2017; 7:45389. <https://doi.org/10.1038/srep45389> PMID: 28358005
12. Chapman KSR, Hatch MD. Regulation of C₄ photosynthesis: Mechanism of activation and inactivation of extracted pyruvate, inorganic phosphate dikinase in relation to dark/light regulation. *Archives of Biochemistry and Biophysics*. 1981; 210(1):82–89. [https://doi.org/10.1016/0003-9861\(81\)90166-1](https://doi.org/10.1016/0003-9861(81)90166-1) PMID: 6271074
13. Ashton AR, Burnell JN, Hatch MD. Regulation of C₄ photosynthesis: Inactivation of pyruvate, Pi dikinase by ADP-dependent phosphorylation and activation by phosphorolysis. *Archives of Biochemistry and Biophysics*. 1984; 230(2):492–503. [https://doi.org/10.1016/0003-9861\(84\)90429-6](https://doi.org/10.1016/0003-9861(84)90429-6) PMID: 6324689
14. Chastain CJ, Chollet R. Regulation of pyruvate, orthophosphate dikinase by ADP-/Pi-dependent reversible phosphorylation in C₃ and C₄ plants. *Plant Physiology and Biochemistry*. 2003; 41(6-7):523–532. [https://doi.org/10.1016/S0981-9428\(03\)00065-2](https://doi.org/10.1016/S0981-9428(03)00065-2)
15. Astley HM, Parsley K, Aubry S, Chastain CJ, Burnell JN, Webb ME, et al. The pyruvate, orthophosphate dikinase regulatory proteins of Arabidopsis are both bifunctional and interact with the catalytic and nucleotide-binding domains of pyruvate, orthophosphate dikinase. *The Plant journal: for cell and molecular biology*. 2011; 68(6):1070–80. <https://doi.org/10.1111/j.1365-313X.2011.04759.x>
16. Chen YB, Lu TC, Wang HX, Shen J, Bu TT, Chao Q, et al. Posttranslational Modification of Maize Chloroplast Pyruvate Orthophosphate Dikinase Reveals the Precise Regulatory Mechanism of Its Enzymatic Activity. *Plant physiology*. 2014; 165(2):534–549. <https://doi.org/10.1104/pp.113.231993> PMID: 24710069
17. Jiang L, Chen YB, Zheng J, Chen Z, Liu Y, Tao Y, et al. Structural Basis of Reversible Phosphorylation by Maize Pyruvate Orthophosphate Dikinase Regulatory Protein. *Plant physiology*. 2016; 170(2):732–41. <https://doi.org/10.1104/pp.15.01709> PMID: 26620526

18. Kang HG, Park S, Matsuoka M, An G. White-core endosperm floury endosperm-4 in rice is generated by knockout mutations in the C₄-type pyruvate orthophosphate dikinase gene (OsPPDKB). *The Plant Journal*. 2005; 42(6):901–911. <https://doi.org/10.1111/j.1365-313X.2005.02423.x> PMID: 15941402
19. Chastain CJ, Failing CJ, Manandhar L, Zimmermann MA, Lakner MM, Nguyen THT. Functional evolution of C₄ pyruvate, orthophosphate dikinase. *Journal of Experimental Botany*. 2011; 62(9):3083–3091. <https://doi.org/10.1093/jxb/err058> PMID: 21414960
20. Doyle JR, Burnell JN, Haines DS, Llewellyn LE, Motti Ca, Tapiolas DM. A rapid screening method to detect specific inhibitors of pyruvate orthophosphate dikinase as leads for C₄ plant-selective herbicides. *Journal of biomolecular screening*. 2005; 10(1):67–75. <https://doi.org/10.1177/1087057104269978> PMID: 15695345
21. Haines DS, Burnell JN, Doyle JR, Llewellyn LE, Motti CA, Tapiolas DM. Translation of in vitro inhibition by marine natural products of the C₄ acid cycle enzyme pyruvate Pi dikinase to *in vivo* C₄ plant tissue death. *Journal of Agricultural and Food Chemistry*. 2005; 53(10):3856–3862. <https://doi.org/10.1021/jf048010x> PMID: 15884807
22. Motti CA, Bourne DG, Burnell JN, Doyle JR, Haines DS, Liptrot CH, et al. Screening marine fungi for inhibitors of the C₄ plant enzyme pyruvate phosphate dikinase: Unguinol as a potential novel herbicide candidate. *Applied and Environmental Microbiology*. 2007; 73(6):1921–1927. <https://doi.org/10.1128/AEM.02479-06> PMID: 17220253
23. Motti CA, Bourguet-Kondracki ML, Longeon A, Doyle JR, Llewellyn LE, Tapiolas DM, et al. Comparison of the biological properties of several marine sponge-derived sesquiterpenoid quinones. *Molecules*. 2007; 12(7):1376–1388. <https://doi.org/10.3390/12071376> PMID: 17909493
24. Wu C, Dunaway-Mariano D, Mariano PS. Design, synthesis, and evaluation of inhibitors of pyruvate phosphate dikinase. *Journal of Organic Chemistry*. 2013; 78(5):1910–1922. <https://doi.org/10.1021/jo3018473> PMID: 23094589
25. Armstrong JI, Portley AR, Chang YT, Nierengarten DM, Cook BN, Bowman KG, et al. Discovery of carbohydrate sulfotransferase inhibitors from a kinase- directed library. *Angewandte Chemie—International Edition*. 2000; 39(7):1303–1306. [https://doi.org/10.1002/\(SICI\)1521-3773\(20000403\)39:7%3C1303::AID-ANIE1303%3E3.0.CO;2-0](https://doi.org/10.1002/(SICI)1521-3773(20000403)39:7%3C1303::AID-ANIE1303%3E3.0.CO;2-0) PMID: 10767039
26. Salahas G, Manetas Y, Gavalas NA. Assaying for pyruvate, orthophosphate dikinase activity: Necessary precautions with phospho enolpyruvate carboxylase as coupling enzyme. *Photosynthesis Research*. 1990; 24(2):183–188. PMID: 24419911
27. R Core Team. R: A Language and Environment for Statistical Computing; 2004. R Foundation for Statistical Computing, Vienna, Austria. url: <https://www.R-project.org/>
28. Ritz C, Baty F, Streibig JC, Gerhard D. Dose-Response Analysis Using R. *PLOS ONE*. 2016; 10(12): e0146021. <https://doi.org/10.1371/journal.pone.0146021>
29. Akaike H. A New Look at the Statistical Model Identification. *IEEE Transactions on Automatic Control*. 1974; 19(6):716–723. <https://doi.org/10.1109/TAC.1974.1100705>
30. Aho K, Derryberry D, Peterson T. Model selection for ecologists: The worldviews of AIC and BIC. *Ecology*. 2014; 95(3):631–636. <https://doi.org/10.1890/13-1452.1> PMID: 24804445
31. Burnell JN, Hatch MD. Photosynthesis in phosphoenolpyruvate carboxykinase-type C₄ plants: Photosynthetic activities of isolated bundle sheath cells from *Urochloa panicoides*. *Archives of Biochemistry and Biophysics*. 1988; 260(1):177–186. [https://doi.org/10.1016/0003-9861\(88\)90440-7](https://doi.org/10.1016/0003-9861(88)90440-7) PMID: 3124745
32. Arnon DI. Copper enzymes in isolated chloroplasts. Polyphenoloxidase in *Beta vulgaris*. *Plant Physiology*. 1949; 24(1):1–15. <https://doi.org/10.1104/pp.24.1.1> PMID: 16654194
33. Shapovalov MV, Dunbrack RL. A smoothed backbone-dependent rotamer library for proteins derived from adaptive kernel density estimates and regressions. *Structure*. 2011; 19(6):844–858. <https://doi.org/10.1016/j.str.2011.03.019> PMID: 21645855
34. Pettersen EF, Goddard TD, Huang CC, Couch GS, Greenblatt DM, Meng EC, et al. UCSF Chimera—A visualization system for exploratory research and analysis. *Journal of Computational Chemistry*. 2004; 25(13):1605–1612. <https://doi.org/10.1002/jcc.20084> PMID: 15264254
35. RDKit: Open-source cheminformatics; 2016. url: <http://www.rdkit.org>
36. Trott O, Olson AJ. Software news and update AutoDock Vina: Improving the speed and accuracy of docking with a new scoring function, efficient optimization, and multithreading. *Journal of Computational Chemistry*. 2010; 31(2):455–461. <https://doi.org/10.1002/jcc.21334> PMID: 19499576
37. Koes DR, Baumgartner MP, Camacho CJ. Lessons learned in empirical scoring with smina from the CSAR 2011 benchmarking exercise. *Journal of Chemical Information and Modeling*. 2013; 53(8):1893–1904. <https://doi.org/10.1021/ci300604z> PMID: 23379370
38. Schrödinger LLC. The PyMOL Molecular Graphics System, Version 1.8; 2015.

39. Toullec D, Pianetti P, Coste H, Bellevergue P, Grand-Perret T, Ajakane M, et al. The bisindolylmaleimide GF 109203X is a potent and selective inhibitor of protein kinase C. *Journal of Biological Chemistry*. 1991; 266(24):15771–15781. PMID: [1874734](#)
40. Davis PD, Hill CH, Lawton G, Nixon JS, Wilkinson SE, Hurst SA, et al. Inhibitors of protein kinase C. 1. 2,3-bisarylmaleimides. *Journal of Medicinal Chemistry*. 1992; 35(1):177–184. <https://doi.org/10.1021/jm00079a024> PMID: [1732526](#)
41. Martiny-Baron G, Kazanietz MG, Mischak H, Blumberg PM, Kochs G, Hug H, et al. Selective inhibition of protein kinase C isozymes by the indolocarbazole Gö 6976. *Journal of Biological Chemistry*. 1993; 268(13):9194–9197. PMID: [8486620](#)
42. Tanaka M, Sagawa S, Hoshi Ji, Shimoma F, Matsuda I, Sakoda K, et al. Synthesis of anilino-monoindolylmaleimides as potent and selective PKC β inhibitors. *Bioorganic & medicinal chemistry letters*. 2004; 14(20):5171–4. <https://doi.org/10.1016/j.bmcl.2004.07.061>
43. Leclerc S, Garnier M, Hoessel R, Marko D, Bibb JA, Snyder GL, et al. Indirubins inhibit glycogen synthase kinase-3 β and CDK5/P25, two protein kinases involved in abnormal tau phosphorylation in Alzheimer's disease. A property common to most cyclin-dependent kinase inhibitors? *Journal of Biological Chemistry*. 2001; 276(1):251–260. <https://doi.org/10.1074/jbc.M002466200> PMID: [11013232](#)
44. Meijer L, Skaltsounis AL, Magiatis P, Polychronopoulos P, Knockaert M, Leost M, et al. GSK-3-Selective Inhibitors Derived from Tyrian Purple Indirubins. *Chemistry and Biology*. 2003; 10(12):1255–1266. <https://doi.org/10.1016/j.chembiol.2003.11.010> PMID: [14700633](#)
45. Albert DH, Tapang P, Magoc TJ, Pease LJ, Reuter DR, Wei RQ, et al. Preclinical activity of ABT-869, a multitargeted receptor tyrosine kinase inhibitor. *Molecular cancer therapeutics*. 2006; 5(4):995–1006. <https://doi.org/10.1158/1535-7163.MCT-05-0410> PMID: [16648571](#)
46. García-Echeverría C. Allosteric and ATP-competitive kinase inhibitors of mTOR for cancer treatment. *Bioorganic and Medicinal Chemistry Letters*. 2010; 20(15):4308–4312. <https://doi.org/10.1016/j.bmcl.2010.05.099> PMID: [20561789](#)
47. Tice CM. Selecting the right compounds for screening: does Lipinski's Rule of 5 for pharmaceuticals apply to agrochemicals?. *Pest Management Science*. 2001; 57(1):3–16. [https://doi.org/10.1002/1526-4998\(200101\)57:1%3C3::AID-PS269%3E3.0.CO;2-6](https://doi.org/10.1002/1526-4998(200101)57:1%3C3::AID-PS269%3E3.0.CO;2-6) PMID: [11455629](#)
48. Greaves B, Poole SC, Hwa CM, Fan JC. Method for inhibition of oxygen corrosion in aqueous systems by the use of a tannin activated oxygen scavenger. US Patent 5,587,109. 1996
49. Grodsky N, Li Y, Bouzida D, Love R, Jensen J, Nodes B, et al. Structure of the catalytic domain of human protein kinase C β II complexed with a bisindolylmaleimide inhibitor. *Biochemistry*. 2006; 45(47):13970–13981. <https://doi.org/10.1021/bi061128h> PMID: [17115692](#)
50. Takimura T, Kamata K, Fukasawa K, Ohsawa H, Komatani H, Yoshizumi T, et al. Structures of the PKC-I kinase domain in its ATP—Bound and apo forms reveal defined structures of residues 533–551 in the C-terminal tail and their roles in ATP binding. *Acta Crystallographica Section D: Biological Crystallography*. 2010; 66(5):577–583. <https://doi.org/10.1107/S0907444910005639>
51. Zhang J, Yang PL, Gray NS. Targeting cancer with small molecule kinase inhibitors. *Nature Reviews Cancer*. 2009; 9(1):28–39. <https://doi.org/10.1038/nrc2559> PMID: [19104514](#)

Copyright of PLoS ONE is the property of Public Library of Science and its content may not be copied or emailed to multiple sites or posted to a listserv without the copyright holder's express written permission. However, users may print, download, or email articles for individual use.